Springer

KSME

Journal of Mechanical Science and Technology 33 (10) (2019) 4813~4821
www.springerlink.com/content/1738-494x(Print)/1976-3824(Online)
DOI 10.1007/s12206-019-0922-9

Creep deformation characteristics of microalloyed HP40Nb steel at 950 °C †

Van Hung Dao, Jung Soo Song*, Joo Yong Kim and Kee Bong Yoon

Department of Mechanical Engineering, Chung-Ang University, 84 Heukseok-ro, Dongjak-gu, Seoul, Korea

(Manuscript Received June 23, 2019; Revised July 18, 2019; Accepted July 22, 2019)

Abstract

In the present work, several specimens were obtained from microalloyed HP40Nb reformer tubes with the different serviced period. The creep tests were conducted at a temperature of 950 °C and under stress levels in the range 25-55 MPa. Results indicated that the degradation of the creep life was due to the increase of the serviced period. The microstructural degradation and creep voids were observed at the grain boundary regions, attributed to the main reason leading to the premature creep failure. The creep exponent started decreasing after the servicing and approached a constant value after 7.2 years. The creep coefficient was obtained to be a function of time when the creep exponent was constant. Norton's creep power law equation was used to derive an equation describing the relationship between the diametrical expansion and serviced period of the reformer tubes. Larson-Miller curves were obtained from creep test data. Amount of carbides from the different serviced period was also calculated.

Keywords: HP40Nb alloy; Reformer tube; Carbide; Creep test; Larson-Miller parameter

1. Introduction

Over the past five decades, reformer tubes of microalloyed HP40Nb—an austenitic heat-resistant alloy—have been manufactured using the centrifugal casting process for high strength and high creep resistance [1]. Therefore, the tubes could be used at high temperatures and under high stresses, and they had a long life span under standard operating conditions. The microstructural features of HP40Nb can be stabilized by adding a microalloying element (Nb and Ti). Microalloying elements have been documented to play an important role in promoting not only the fragmentation and dispersion of hard deformation-resistant carbide particles of the as-cast microstructure but also the partial replacement of chromium (Cr) carbide; they form an MC-type carbide (M: Metal with Nb or Ti), which enhances the creep strength of steel [2-7]. Thus, microalloyed HP40Nb is popular for manufacturing reformer tubes of heating furnaces.

Microalloyed HP40Nb steel has high Cr (25 wt.%) and Ni (35 wt.%) content in its austenitic structure, fulfilling the main requirement for creep-resistant materials. The microstructure consists of primary and secondary carbide (M_7C_3/MC and $M_{23}C_6$) precipitates at the grain boundary regions, which contribute to the high creep resistance of the material [7]. In the early stages of its use, the small carbide particles are the dispersion of secondary carbides in the matrix of austenite grains. They act as a barrier to prevent the propagation of creep damage through the microstructure. In addition, researchers have demonstrated that creep properties of a material can be identified from the metallurgical features of the material, type of distribution of carbides in the material microstructure, and mechanical properties of the material [8, 9].

Reformer tubes operate in extremely harsh environmental conditions [10]. The conditions may include high temperatures, high stresses, and corrosive factors. The failure of reformer tubes has been attributed to creep, which often leads to microstructure destabilization. In particular, the coalescence and coarsening of carbides and the formation of creep voids during service reduce creep deformation [1, 2]. Hence, it should recommend investigating creep on the serviced period for microalloyed HP40Nb steel reformer tubes for better and safer design. In the present work, for experiments, the specimens were used for comparing creep tests at the temperature of 950 °C and for stresses in the range 25-55 MPa. The initial results indicated that the variation in creep properties was related to the serviced period. The levels of microstructural degradation were studied carefully to explain changes in the creep deformation behavior. Furthermore, for a constant creep exponent, the relationship between an increase in the tube diameter and the serviced period was determined based on the creep coefficient, which was identified to be a function of time. The use of the Larson-Miller diagram for assessing predictions of the remaining life is proposed. Furthermore, carbide

*Corresponding author. Tel.: +82 2 8211547
E-mail address: songjs@cau.ac.kr
† Recommended by Editor Chongdu Cho
© KSME & Springer 2019

precipitation is determined to explain the tendency of carbide grains to coarsen.

2. Experimental procedures

2.1 Reformer tube information and specimen preparation

Reformer tubes are mainly manufactured through the centrifugal casting process, and their nominal lifetime is approximately 100000 h (≈11.4 years). They can operate at temperatures up to 950 °C and are designed for internal pressures of 10-40 bars [1]. In this study, reformer tubes were obtained from a furnace containing 72 catalyst-filled vertical tubes arranged in two radiant chambers. These vertical tubes with a length of 14 m were supported at the bottom and free to expand at the top. The outer diameter of each tube was 146.6 mm and the internal diameter was 135.8 mm. The raw materials were metal gas (CH_4) and steam, which entered into the top of reformer tubes from the top end at a temperature of around 755 K and with a pressure in the range 15-17 bars. They flowed downward over the catalyst in the individual tubes before emerging from the bottom end at a temperature of around 1173 K.

The material used in this study was microalloyed HP40Nb, and its chemical composition is presented in Table 1. Virgin specimens were cut from tubes collected from the bottom part outside the furnace. Other specimens were obtained from tubes collected from the heated part of the furnace, and the serviced periods of the tubes were 1.75, 6, and 7.2 years. Detailed information and photographs of the reformer tubes are presented in Table 2 and Fig. 1. These specimens were taken out and brought to the laboratory for examination and analysis.

2.2 Creep test

The creep test specimens were fabricated according to the ASTM E8/E8M standard [11] by wire-cut electrical discharge machining, and their diameter and gage length were 7 and 60 mm from the longitudinal direction of the tubes (see Fig. 1(b)).

The creep test procedure was in accordance with the ASTM E139 standard [12], and the tests were conducted creep testing machines at 950 °C and under stresses in the range 25-55 MPa. The test conditions are summarized in Table 3; a total of 16 creep tests were conducted. Creep curves showing the creep strain as a function of the elapsed time were directly received and plotted on a graph on the computer screen. The creep strain versus time data was converted to creep strain rate versus elapsed time data by using the seven-point incremental method specified in the ASTM E647 standard.

To identify microstructural changes at the grain boundaries, rectangular specimens were cut from the tubes so that they could be held in the hand for microstructure analysis (see Fig. 1(b)). The specimens were ground using silicon carbide papers with a grit size of 320-2400 and water, polished on a cloth with 0.6 and 0.1 μm diamond suspensions, and cleaned

Table 1. Chemical composition of microalloyed HP40Nb according to ASTM A608 (wt.%).

Material	C	Ni	Cr	Nb	Si	Mn	Mo	Fe
Microal-loyed HP40Nb	0.38-0.45	34-37	24-27	0.5-1.5	0.5-1.5	≤1.5	0.50	Bal

Table 2. Detailed information on the reformer tubes.

Tube No.	#17-1	#19	#17-2	#56
Installed	2014	2012.08	2008.01	2008.01
Replaced	2014	2013.12	2013.12	2015.03
Serviced period (years)	0 (virgin)	1.75	6.0	7.2

(a)

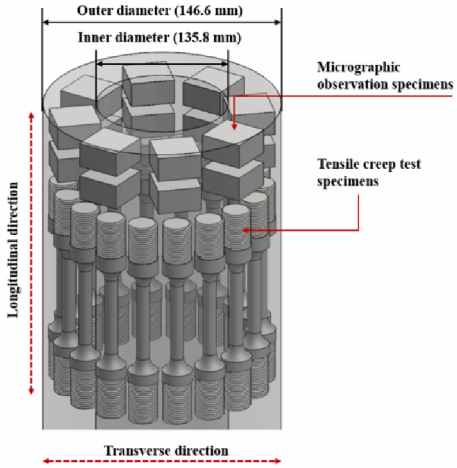

(b)

Fig. 1. (a) Photographs of the reformer tubes; (b) specimen geometry.

using an ultrasonic machine for 2 min in ethanol solution. Finally, they were etched with a solution of 10 % HNO_3, 30 % HCl, and 20 % glycerol. Metallographic characterization was performed using light optical microscopy (LOM) and scanning electron microscopy (SEM), and an energy-dispersive X-ray spectroscopy (EDS) system.

3. Results

3.1 Creep curves and microstructural degradation

Typical creep curves of microalloyed HP40Nb creep tested at a constant temperature of 950 °C and under stresses in the

range 25-55 MPa are shown in Figs. 2(a)-(d). A normal creep curve shows three regions (primary, secondary, and tertiary creep), and the secondary and tertiary creep regions are more dominant than the primary creep region. The steady-state stage is characterized by the secondary creep region. In addition, the creep life often depends strongly on the applied stress and temperature. The tertiary stage marks the start of microstructural degradation. Figs. 3(a)-(d) show plots of creep strain rate versus elapsed time for different stress levels (25-55 MPa); roughly three creep regimes are visible. At the first stage, the creep strain rate initially decreases with an increase in the creep strain. The secondary stage, creep strain rate tends to be constant which is dominant throughout the creep life, and in the final stage, the creep strain rate increased with a further increase in the creep strain. The minimum creep strain rate values were obtained from the secondary creep rate by determining the average value of the strain rate with data in the range of 30 %-60 % of creep rupture time for each specimen, shown in Table 3. These values are also directly proportional to the applied stress, and this relationship is plotted (log-log) in Fig. 4. A, n are creep coefficient and creep exponent values were determined using Norton's power law creep equation, as follows:

$$\dot{\varepsilon} = A\sigma^n . \quad (1)$$

For the serviced periods 0 (virgin), 1.75, 6.0, and 7.2 years, the creep exponent was 11.19, 9.14, 6.40, and 6.28, respectively, confirming that power law hardening decreased with an increase in the serviced period. It should be noted that the creep exponent value of the virgin specimen was considerably higher than the values for the other specimens at 950 °C. The creep exponent values also indicates that the secondary-regime creep deformation in microalloyed HP40Nb is controlled by the dislocation creep mechanism. According to past studies [13-15], while dislocation creep is dominant for creep exponent values in the range 3-12 because of the movement of dislocations, diffusion creep and grain-boundary sliding are dominant for the creep exponent values of 1 and 2, respectively. Fig. 5 depicts the detailed microstructure at two magnifications, ×100 and ×1000, for the different serviced periods for the specimens from the tubes. The virgin microstructure of microalloyed HP40Nb in Fig. 5(a) shows a continuous network of primary carbides forming a dendritic pattern during solidification. However, in the microstructure of the specimen with a serviced period of 1.75 years in Fig. 5(b), a large quantity of small precipitates are observed, they are more apparent at the grain and neighborhood boundaries. The interdendritic carbide content decreased for the serviced periods of 6 and 7.2 years (see Figs. 5(c) and (d)), and the blocky-shaped interdendritic carbides dispersed and formed large granular carbides.

EDS analysis of the virgin specimen, shown in Fig. 6(a), revealed that the white precipitates correspond to Nb-rich carbides that combined with carbon atoms to form fine precipitates of new MC-type carbides (M: Metal with Nb or Ti) that

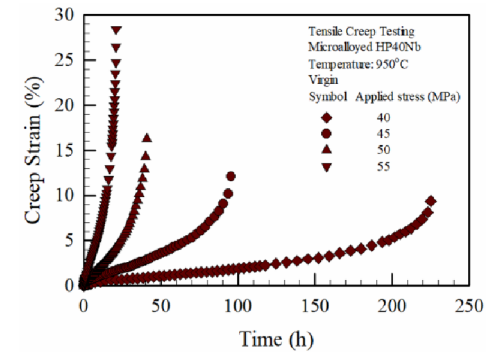

(a) As-cast (virgin)

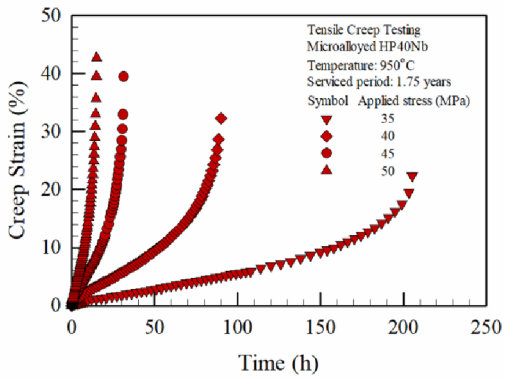

(b) Specimen with serviced period of 1.75 years

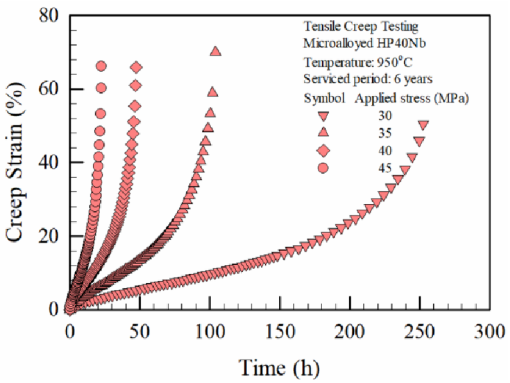

(c) Specimen with serviced period of 6 years

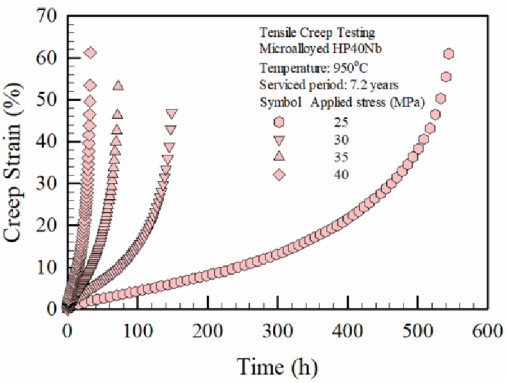

(d) Specimen with serviced period of 7.2 years

Fig. 2. Plot of time versus strain obtained in the creep test at 950 °C for microalloyed HP40Nb under different stresses.

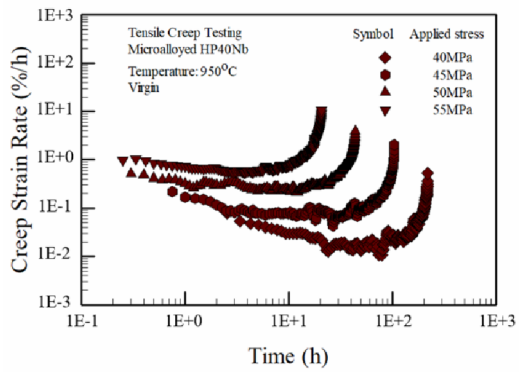

(a) As-cast (virgin)

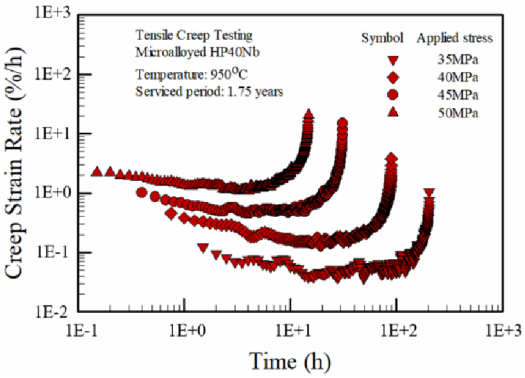

(b) Specimen with serviced period of 1.75 years

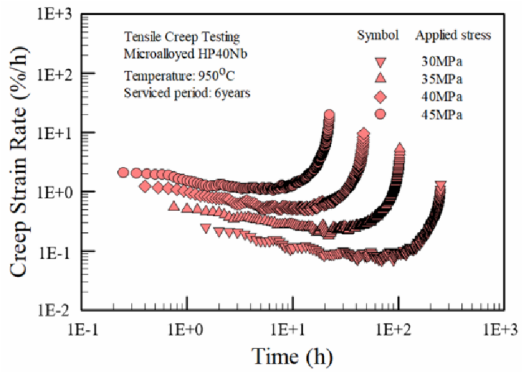

(c) Specimen with serviced period of 6 years

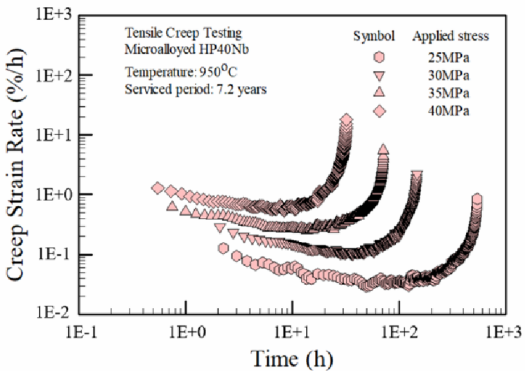

(d) Specimen with serviced period of 7.2 years

Fig. 3. Plot of time versus creep strain rate obtained in the creep test at 950 °C for microalloyed HP40Nb.

Table 3. Parameters obtained at different stress levels for each of the specimens in creep test for microalloyed HP40Nb at 950 °C.

Serviced period (years)	Temperature (°C)	Applied stress (MPa)	Time to rupture (h)	Minimum creep strain rate (%/h)
Virgin	950	40	225.03	2.82E-02
		45	94.48	1.08E-01
		50	40.97	3.45E-01
		55	20.98	1.00E+00
1.75		35	205.41	6.36E-02
		40	90.17	2.11E-01
		45	31.37	6.78E-01
		50	14.98	1.60E+00
6		30	252.43	1.06E-01
		35	103.97	3.08E-01
		40	47.37	6.19E-01
		45	22.63	1.51E+00
7.2		25	554.30	5.24E-02
		30	148.60	1.43E-01
		35	71.92	4.09E-01
		40	32.31	9.83E-01

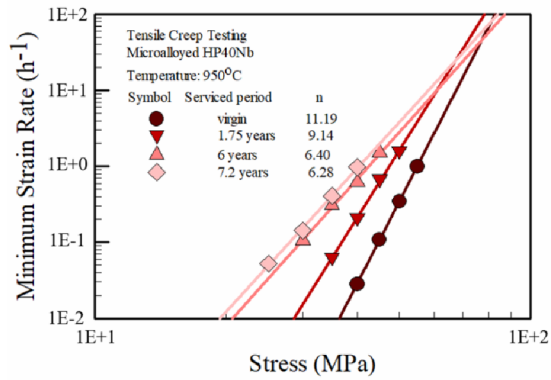

(a)

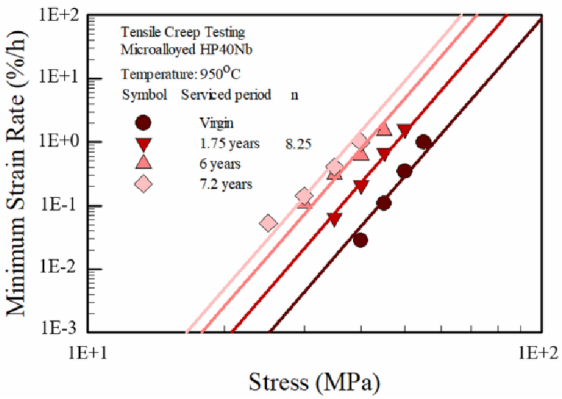

(b)

Fig. 4. Relationship of the minimum strain rate with stress and serviced period after the creep testing of microalloyed HP40Nb specimens: (a) Before; (b) after retaining n value as a constant.

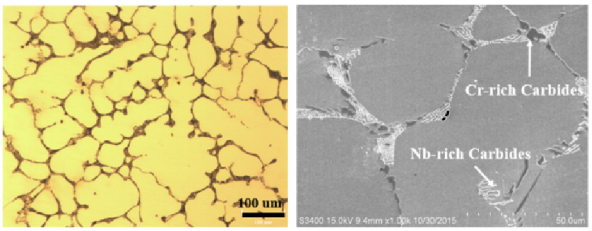

(a) As-cast (virgin)

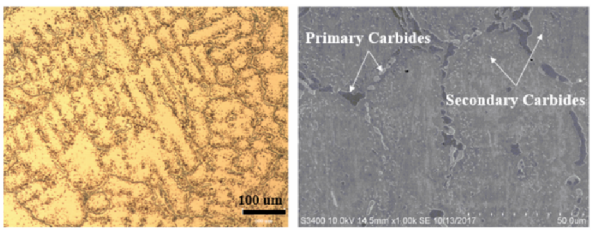

(b) Specimen with serviced period of 1.75 years

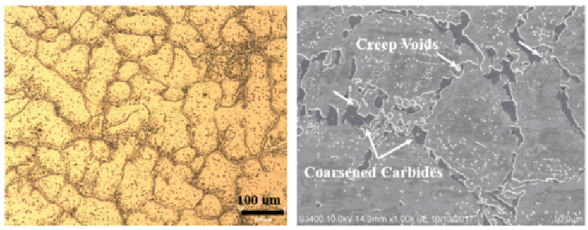

(c) Specimen with serviced period of 6.0 years

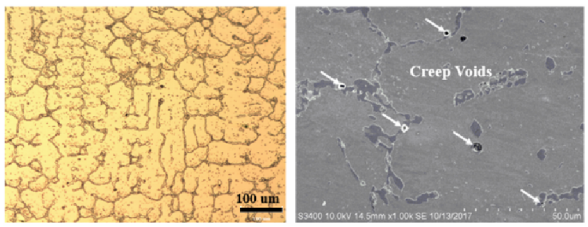

(d) Specimen with serviced period of 7.2 years.

Fig. 5. LOM and SEM images of the surface of microalloyed HP40Nb for the specimens with different serviced periods (magnifications of ×100 and ×1000).

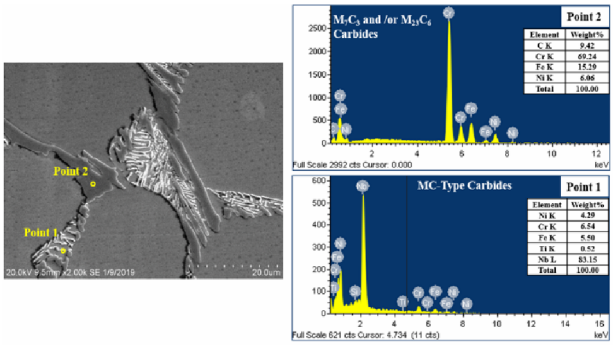

(a) Virgin specimen

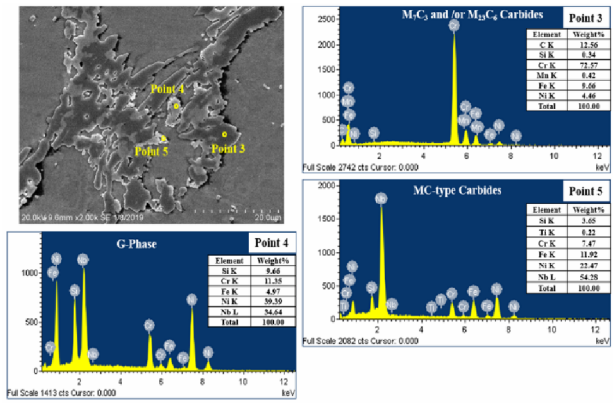

(b) Serviced specimen (7.2 years)

Fig. 6. EDS analysis results for the dark and bright carbide precipitate region.

are stable at high temperatures (indicated by point 1). Thus, the formation of the fine precipitates enhanced the creep strength. By contrast, the precipitates in black contrast could be identified as Cr-rich carbides (M_7C_3 and/ or $M_{23}C_6$; M: Metal with high Cr content) (indicated by point 2) that have adverse effects on the mechanical properties of the material [1, 2, 8]. For long serviced periods, the transformation of primary carbides into secondary carbides is detected in EDS analysis, as shown in Fig. 6(b). The transformation from the initial M_7C_3 carbides into $M_{23}C_6$ at the grain boundaries can be observed mainly in the case of Cr-rich carbides with dark grey precipitates (indicated by point 3), while the observation of Nb-rich carbides with some amount of nickel and silicon suggests that the primary carbide MC (NbC) tends to transform into G-phase, which consists of $Ni1_6Nb_6Si_7$ (indicated by point 4). In particular, (NbTi)C carbides are more stable than NbC (indicated by point 5), as reported in a previous study [4].

The microstructural changes highlighted the progressive reduction in the material's stress resistance capability; this reduction is termed creep damage. The results of the creep tests performed for a constant temperature of 950 °C and a stress level of 40 MPa for all specimens showed that damage growth manifests as an increase in the minimum creep rate during secondary creep and decreases the rupture time (see Table 3). Results showed the creep deformation decreasing with an increase in the serviced period; this finding also confirmed that the creep exponent values could show little change and remain constant after 7.2 years, as shown in Fig. 4(a). This observation is important for deriving the relation between the diameter extension and the serviced period for predicting as well as evaluating the residual life of reformer tubes. Fig. 4(b) shows plots of the minimum creep rate versus stress level for a creep exponent of 8.25, which is the average of the creep exponent values for all the specimens, and a high R^2 value of 0.98. The creep coefficient A was 2.78×10^{-15}, 1.36×10^{-14}, 4.70×10^{-14}, and 8.85×10^{-14} for the serviced periods 0 (virgin), 1.75, 6.0, and 7.2 years. The relation between the creep coefficient and the serviced period obtained in this study was a second order polynomial equation, and the accuracy expressed in terms of the coefficient of determination (R^2) was 0.9743; the relation is nonlinear and the relation obtained is as follows:

$$Log_{10} A = -0.0223 t_S^2 + 0.3509 t_S - 14.5060 \quad (2)$$

where t_S is the serviced period of the tube (in years). This equation was derived using data for the serviced period range 0-7.2 years, and it can be used to predict the creep coefficient. In practice, one of the main reasons for changing the tube diameter is the hydrocarbon cracking reaction that occurs under high-temperature conditions and the stress concentration results from internal pressure. In general, in most cases, tube destruction occurs as a result of strain propagation in the longitudinal direction. The tangential and radial stress are illustrated by Lame's equation, can be expressed as follows for exclusively considering the effect of the internal pressure on tube failure:

$$\sigma_\theta = \frac{r_i^2 P_i - r_o^2 P_o}{r_o^2 - r_i^2} + \frac{(P_i - P_o) r_i^2 r_o^2}{(r_o^2 - r_i^2) r^2} \quad (3)$$

$$\sigma_r = \frac{r_i^2 P_i - r_o^2 P_o}{r_o^2 - r_i^2} - \frac{(P_i - P_o) r_i^2 r_o^2}{(r_o^2 - r_i^2) r^2} \quad (4)$$

where σ_θ and σ_r are the tangential and radial stress at a point on the tube wall; these stresses are directed circumferentially and radially, respectively [16]. The maximum and minimum stress values are identified at $r = r_i$ and $r = r_o$, respectively, where r_i and r_o are the internal and external radii of the tube (in millimeters). P_i and P_o denote the internal and external pressure (in megapascals), it is considered that $P_o = 0$. Eqs. (3) and (4) indicate that the strong influence of the tube diameter on the equivalent stress should be determined based on Tresca theory [17]; this influence is described by Eq. (5) below.

$$\sigma = \sigma_\theta - \sigma_r = \frac{2 P_i r_i^2 r_o^2}{(r_o^2 - r_i^2) r^2}. \quad (5)$$

From a microstructural viewpoint, the authors of a past study [18] observed that the stress concentration usually causes the condensation of atomic vacancies by breaking down the sustainable network structure, and the condensation of vacancies significantly affects creep voids formation. Thus, void formation is strongly dependent on stress.

The integration of Eq. (1) was performed to describe the relationship between diameter extension and serviced period.

$$\int_{\varepsilon_o}^{\varepsilon_s} d\varepsilon = \int_{t_o}^{t_s} A(t).\sigma^n dt. \quad (6)$$

here, ε is the diameter extension (in percentage), and σ is the equivalent stress (in megapascals). Substituting Eq. (5) into Eq. (6) gives the following equation:

$$\int_{\varepsilon_o}^{\varepsilon_s} d\varepsilon = \int_{t_o}^{t_s} A(t).\left[\frac{2 P_i r_i^2 r_o^2}{(r_o^2 - r_i^2) r^2}\right]^n dt. \quad (7)$$

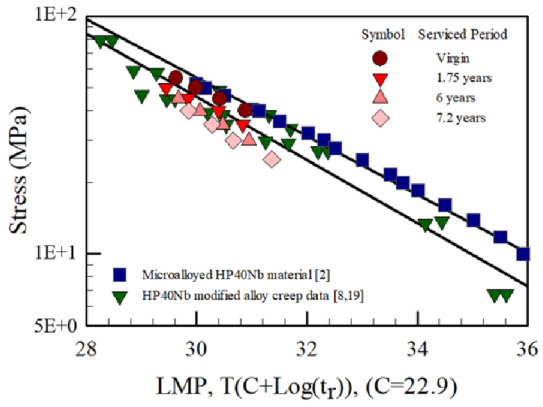

Fig. 7. Larson-Miller diagram for microalloyed HP40Nb with C = 22.9.

From Eq. (7), the relationship between diameter extension and serviced period (year) can be studied by considering the equivalent stress distribution and the creep coefficient as functions of time. Recently, many researchers have conducted failure analysis of serviced exposed primary reformer tubes made of microalloyed HP40Nb steel. They measured and calculated tube diameters extremely precisely to obtain the maximum limits preceding tube failure [19]. In a couple of past studies [2, 20], the authors found that all failed tubes showed a large longitudinal crack that opened up over a length of 300 to 880 mm. The diameter extension is in the range 3 %-4.5 % which can be considered as the standard for replacing tube components for avoiding the risk of damage to the entire system and the time to rupture can be obtained from Eq. (7).

3.2 Creep life measurement by using Larson-Miller curve

The Larson-Miller curve is extensively used in industries to predict the creep life of materials since remaining-life assessment is important for choosing the right material for certain engineering applications. In the most extreme instances, it helps prevent component failure, which could otherwise lead to catastrophic effects. In most engineering applications, it is necessary to choose materials and design components by considering creep damage. The prediction of the creep life of components subjected to high temperatures is necessary to avoid catastrophic effects.

The Larson-Miller curve shown in Fig. 7 was obtained from an analysis of the results of creep tests in Table 3. The remaining creep life was calculated using the Larson-Miller parameter (LMP) curve and substituting the stress rupture time obtained in each test in the LMP equation, which is given by:

$$P = (T + 273) \times (22.9 + \text{Log } t_r) \quad (8)$$

where P is the LMP parameter, t_r is the stress rupture time, T is the temperature (in kelvin), and C = 22.9 is the Larson-Miller constant. Comparison of the curves (shown in Fig. 7)

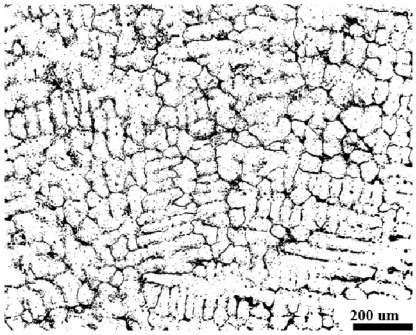

(a) Specimen with serviced period of 1.75 years

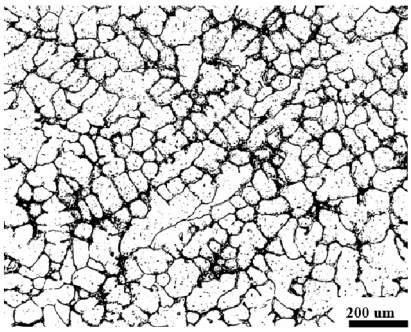

(b) Specimen with serviced period of 6 years

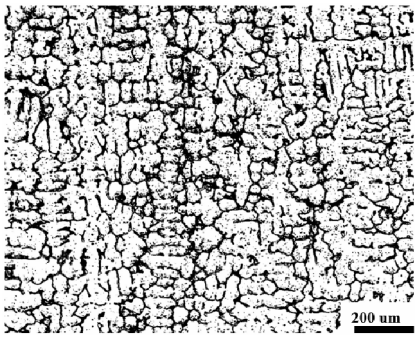

(c) Specimen with serviced period of 7.2 years

Fig. 8. Images analysis on the surface of microalloyed HP40Nb for the specimens with different serviced periods (magnifications of ×50).

for manufacturer data [2], previously reported creep life values [8, 19], and the virgin and serviced period specimens lead to the following inferences:

Creep test results for the virgin specimen were within the limits of the manufacturer data. The curve for the virgin specimen is located above that for previously reported creep test values for a HP40Nb modified material The superior creep properties of microalloyed HP40Nb was obtained which allows to manufacture tubes with thinner wall or, larger diameter. The creep properties can be explained by the presence of the microelement Ti in microalloyed HP40Nb; the microelement enhances the creep property [1, 2, 7, 21, 22].

The curves for the specimens with serviced periods of 1.75, 6, and 7.2 years are below the virgin and manufacturer creep curves. This is because of creep damage accumulated in the specimens, and it will be discussed in a later section.

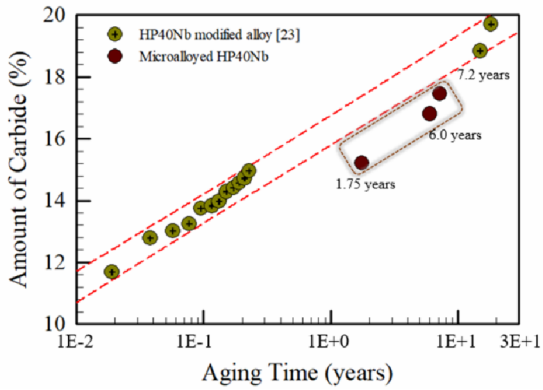

Fig. 9. Influence of serviced period on amount of carbide of microalloyed HP40Nb for the specimens with different serviced periods.

3.3 Amount of carbides measurement

The microstructure of the specimens was observed at relatively low magnification (×50). The morphology of the carbides at the grain boundaries could be seen and their characteristics could be accurately analyzed by the image analysis method, as shown in Figs. 8(a)-(c). For the serviced periods 1.75, 6.0, and 7.2 years, amount of carbides was 15.21 %, 16.83 %, and 17.78 %, respectively. The result indicated that the carbides increased with the serviced period. This explains why the coarsening of carbides became clear after a long serviced period. This result is in agreement with the result of a past study [23].

4. Discussion

The creep exponent tends to be influenced by microstructural degradation, which results from the coalescence and coarsening of primary and secondary carbides, as shown in Fig. 5. The precipitate of small carbide particles at the interdendritic interface could be explained by the transformation of primary carbides into intergranular- or intragranular-type secondary carbides. The small secondary carbide particles formed acted as a barrier, preventing creep deformation, and the creep strength of microalloyed HP40Nb increased. Similar results have been reported previously [9, 24]. The microstructural changes appeared to reach saturation because of the coalescence and coarsening of carbides being dominant for these serviced periods. In addition, creep voids occurred, which can be verified from material degradation resulting from high operating temperatures [20, 25, 26]. This occurrence is a prerequisite for microcracking and the propagation of macrocracks. Furthermore, high-temperature operation (above 950 °C) for prolonged durations accompanied by internal pressure concentration can lead to microstructural changes and severe damage to structural tube components as a result of temperature-sensitive plastic deformation and surface degradation processes. Consequently, the creep resistance is reduced. Similar results were obtained in a previous report [2]. Also, the degree of coarsening of grain boundaries should be

proportional to the serviced period or temperature. It is also consistent with previous results [23, 27, 28].

Fig. 9 also shows a comparison of the amount of carbides between the specimens of this study and a HP40Nb modified material of a previous study at the temperature of 900 °C [23]. Apparently, amount of carbides in HP40Nb steel is greater than that in microalloyed HP40Nb containing titanium. This can be explained a follows. The addition of titanium possibly controls and restrains the coarsening. Moreover, titanium atoms remain in their positions without changing the crystalline volume during the transformation of carbides under high temperatures in the microalloyed material. In the EDS analysis, as shown in Fig. 6, a small amount of Ti (0.52; 0.22 wt.%) was detected on the white precipitates, which included fine precipitation of the new MC-type carbides ((NbTi)C); the presence of Ti appears to have enhanced the creep properties. Similar arguments have been presented in previous studies [1, 2, 7, 21, 22]. In other words, the carbide content is depended on the serviced period, which ranges from 1.75-7.2 years. The remaining life of tubes after the serviced period should probably be evaluated after the amount of carbides of the tube is determined.

5. Conclusions

Variations in the creep behavior at the temperature of 950 °C, remaining life assessment, and the carbide precipitate of microalloyed HP40Nb steel for different service periods were investigated. The following conclusions were obtained:

(1) On the basis of microstructural degradation with the serviced period, creep life and creep deformation were reduced. The creep exponent was found in the range of 6.28-11.19, indicated the existence of the dislocation creep mechanism in microalloyed HP40Nb steel.

(2) The creep exponent decreased non-linearly and it was constant for serviced periods of 7.2 years under different stresses at 950 °C. For a constant creep exponent value of 8.25, the creep coefficient was a function of time. The equation proposed for predicting the diameter extension (%) and serviced period (year) was used to assess the residual life of tube components.

(3) Larson-Miller curves were plotted by using most of the test data obtained in this study. The results indicated the superior creep properties of microalloyed HP40Nb compared to that of HP40Nb modified which allows to manufacture tubes with lower thin wall and/or larger diameter. Also, the curves are in good agreement with the general tendency of standard curves documented in the literature. Amount of carbides determined to be 15.21 %, 16.83 %, 17.78 % with serviced periods of 1.75, 6, and 7.2 years, respectively. It explained the tendency of carbide grains to coarsen.

Acknowledgments

This work was supported by the KETEP (No. 2013 2010 500060), granted financial resource from the Ministry of Trade, Industry & Energy (MOTIE), Republic of Korea. This work was also supported by the KETEP granted from MOTIE (No. 20141010101850). Authors deeply appreciate the company providing the serviced reformer tubes and relevant information.

Nomenclature

A	: Creep coefficient
C	: Larson-Miller constant
n	: Creep exponent
σ	: Applied stress
$\dot{\varepsilon}$	: Minimum creep strain rate
P	: Pressure
P_o	: External pressure
P_i	: Internal pressure
r	: Radii of tube
r_o	: External radii of tube
r_i	: Internal radii of tube
R^2	: Coefficient of determination
T	: Temperature
t_S	: Serviced period
t_r	: Rupture time

References

[1] L. Bonaccorsi, E. Guglielmino, R. Pino, C. Servetto and A. Sili, Damage analysis in Fe-Cr-Ni centrifugally cast alloy tubes for reforming furnaces, *Engineering Failure Analysis,* 36 (2014) 65-74.

[2] J. Swaminathan, K. Guguloth, M. Gunjan, P. Roy and R. Ghosh, Failure analysis and remaining life assessment of service exposed primary reformer heater tubes, *Engineering Failure Analysis*, 15 (2008) 311-331.

[3] A. R. Andrade, C. Bolfarini, L. A. M. Ferreira, A. A. A. Vilar, C. D. Souza Filho and L. H. C. Bonazzi, Influence of niobium addition on the high temperature mechanical properties of a centrifugally cast HP alloy, *Materials Science and Engineering A*, 628 (2015) 176-180.

[4] L. H. de Almeida, A. F. Ribeiro and I. Le May, Microstructural characterization of modified 25Cr-35Ni centrifugally cast steel furnace tubes, *Materials Characterization*, 49 (2002) 219-229.

[5] Y. Zhang, Y. Sun, S. Guan, X. Deng and X. Yan, Effect of titanium and tungsten on the structure and properties of heat-abrasion resistant steel, *Materials Science and Engineering A,* 478 (1-2) (2008) 214-220.

[6] G. Pilloni, E. Quadrini and S. Spigarelli, Interpretation of the role of forest dislocations and precipitates in high-temperature creep in a Nb-stabilised austenitic stainless steel, *Materials Science and Engineering A,* 279 (1) (2000) 52-60.

[7] A. Alvino, D. Ramires, A. Tonti and D. Lega, Influence of chemical composition on microstructure and phase evolution of two HP heat resistant stainless steels after long term plant-service aging, *Material at High Temperature*, 31 (1) (2014) 2-11.

[8] R. Voicu, J. Lacaze, E. Andrieu, D. Poquillon and J. Furtado, Creep and tensile behaviour of austenitic Fe-Cr-Ni stainless steels, *Materials Science and Engineering A,* 510 (2009) 185-189.
[9] D. Alessio, G. Gonzalez, V. F. Pirrone, L. Iurman and L. Moro, Variation of creep properties in HP steel by influence of temperature, *Procedia Materials Science*, 1 (2012) 104-109.
[10] J. Lee, J. H. Han, J. H. Moon, C. H. Jeong, M. Kim, J. Y. Kim and S. H. Lee, Characteristics of heat transfer and chemical reaction of methane-steam reforming in a porous catalytic medium, *Journal of Mechanical Science and Technology*, 30 (1) (2016) 473-481.
[11] *ASTM Standard E8.8M*, Standard test methods for tension testing of metallic materials.
[12] *ASTM3-01-E139*, Standard test method for conducting creep, creep-rupture, and stress-rupture test of metallic materials.
[13] S. Latha, M. D. Mathew, P. Parameswaran, K. B. S. Rao and S. L. Mannan, Thermal creep properties of alloy D9 stainless steel and 316 stainless steel fuel clad tubes, *Int. of Pressure Vessels and Piping*, 85 (2008) 866-870.
[14] A. Ghatak and P. S. Robi, A comparative study of constitutive equations for the creep deformation of HP40Nb micro-alloyed steel, *Materials Science and Engineering A,* 648 (2015) 418-427.
[15] A. Ghatak and P. S. Robi, High-temperature deformation behavior of HP40Nb micro-alloyed reformer steel, *Metallography, Microstructure and Analysis,* 4 (6) (2015) 508.
[16] B. N. Phalguna, Stress and failure analysis of thick walled cylinder with oblique hole, *Int. Journal of Engineering Research and Technology*, 6 (2017) 2278-0181.
[17] *https://en.wikipedia.org/wiki/Henri_Tresca*.
[18] W. D. Nix, Introduction to the viewpoint set on creep cavitation, *Scripta Metallurgica*, 17 (1983) 1-4.
[19] E. Guglielmino, R. Pino, C. Servetto and A. Sili, *Handbook of Materials Failure Analysis with Case Studies from the Chemicals, Concrete and Power Industries*, Elsevier Ltd. (2016) 69-91.
[20] A. K. Ray, S. K. Sinha, Y. N. Tiwari, J. Swaminathan, G. Das, S. Chaudhuri and R. Singh, Analysis of failed reformer tubes, *Engineering Failure Analysis,* 10 (3) (2003) 351-362.
[21] A. R. Andrade, C. Bolfarini, L. A. M. Ferreira, C. D. Souza Filho and L. H. C. Bonazzi, Titanium micro addition in a centrifugally cast HPNb alloy: High temperature mechanical properties, *Materials Science and Engineering A*, 636 (2015) 48-52.
[22] B. Piekarski, Effect of Nb and Ti additions on microstructure, and identification of precipitates in stabilized Ni-Cr cast austenitic steels, *Materials Characterization*, 47 (2001) 181-186.
[23] C. J. Liu and Y. Chen, Variations of the microstructure and mechanical properties of HP40Nb hydrogen reformer tube with time at elevated temperature, *Materials and Design*, 32 (4) (2011) 2507-2512.
[24] M. H. Shariat, A. H. Faraji, A. Ashraf Riahy and M. M. Alipour, In advances creep failure of HP modified reformer tubes in an ammonia plant, *Journal Corrosion Science and Engineering* (2003).
[25] K. B. Yoon and D. G. Jeong, Oxidation failure of radiant heater tubes, *Engineering Failure Analysis*, 6 (2) (1999) 101-112.
[26] W. Z. Wang, F. Z. Xuan, Z. D. Wang, B. Wang and C. J. Liu, Effect of overheating temperature on the microstructure and creep behavior of HP40Nb alloy, *Material and Design*, 32 (7) (2011) 4010-4016.
[27] V. H. Dao, K. B. Yoon, G. Yang and J. S. Oh, Determination of creep constitutive model for 28-48WCo alloy based on experimental creep tests at 817-982 °C, *Journal of Mechanical Science and Technology*, 32 (2018) 4201-4208.
[28] J. M. Gong, S. T. Tu and K. B. Yoon, Damage assessment and maintenance strategy of hydrogen reformer furnace tubes, *Engineering Failure Analysis*, 6 (1999) 143-153.

Van Hung Dao received his M.S degree in Mechanical Engineering from Chung-Ang University, Korea in 2016. He is currently a Ph.D. candidate at Chung-Ang University. His research interests are microstructural analysis and application of high temperature fracture mechanics to life assessment of structural material. He is extending research to behavior of additive manufactured materials.

Jung Soo Song received his Master degree in Mechanical Engineering from Chung-Ang University, Korea in 2002. He is currently a Ph.D. candidate at Chung-Ang University. And he is also a Senior Researcher in Energy Safety Research Institute at Chung-Ang University. His research interests are high temperature fracture mechanics, remaining life assessment and risk-based inspection for industrial facilities.

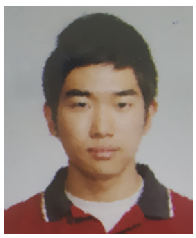

Joo Yong Kim received his M.S. degree in Mechanical Engineering from Chung-Ang University, Korea in 2016. He is now working on Korea Company. His research interests are microstructural analysis, reliability and life assessment of structural material such as reformer tube.

Kee Bong Yoon received his M.S. in Mechanical Engineering from KAIST and Ph.D. from Georgia Institute of Technology. He is currently a Professor at Chung-Ang University. His research interests are high temperature fracture mechanics, failure analysis and risk based management of facilities in semiconductor industry as well as the conventional power and process plants. He is extending research to fracture of additive manufactured materials.